The reaction antigorite → olivine + talc + H_2O in the Bergell aureole, N. Italy

R. H. WORDEN*, G. T. R. DROOP AND P. E. CHAMPNESS

Department of Geology, The University of Manchester, Oxford Road, Manchester M13 9PL, U.K.

Abstract

The low-grade contact metamorphic decomposition of antigorite serpentine to olivine and talc has been studied using TEM. The reaction was more complex than has been assumed by previous workers in that (i) FeO played a significant role in controlling the temperature of reaction, and (ii) minor amounts of an aluminous phase (chlorite) were probably produced. The reaction occurred over a range of temperatures within which the assemblage antigorite + talc + olivine was stable and the antigorite became progressively more Mg-rich as the reaction proceeded. Oriented nucleation of talc occurred within the antigorite. However, the olivine breakdown product did not require nucleation; rather it appears to have grown on pre-existing olivine grains. Communication between the sites of reaction was probably facilitated by an ubiquitous grain-boundary fluid.

KEYWORDS: antigorite, olivine, talc, TEM, contact metamorphism, Bergell aureole.

Introduction

SEVERAL recent studies have been published in which transmission electron microscopy (TEM) was used for the interpretation of the mechanisms of short-lived, high-temperature metamorphic events (e.g. Brearley 1987; Worden *et al.*, 1987, 1988). Other studies have been concerned with the mechanisms of very high-pressure reactions in metagabbros (e.g. Wayte *et al.*, 1989; Trolliard *et al.*, 1988; Otten and Buseck, 1987). This paper describes the first TEM study of a low-grade contact-metamorphic reaction—the breakdown of antigorite in the aureole of a fairly large intrusion in the Central Alps. The heating rate in this case would have been much lower than in the high-temperature reactions mentioned above. Light optics and electron microprobe analysis were used in addition to TEM to characterise the textures and chemistry of the reaction. This work follows on from that of Mellini *et al.* (1987) who studied the crystal-structural and -chemical changes in antigorite with increasing temperature in samples collected on a traverse towards the igneous contact.

* Present address: BP International Limited, Sunbury Research Centre, Chertsey Road, Sunbury-on-Thames, Middlesex TW16 7LN, U.K.

Geological background

The peridotitic rocks in the Alps have been studied extensively in recent years. The relative simplicity of the chemistry and mineralogy of these rocks makes them ideal for a study of the conditions, controls and mechanisms of metamorphic reactions. The present study concerns the Malenco serpentinite in the Bergell Complex, one of the largest ultramafic bodies in the Alps. Dietrich *et al.* (1974) proposed that the mafic and ultramafic rocks in the Bergell region are remnants of obducted ocean crust. Burkhard and O'Neil (1988) used stable isotopes to demonstrate that the Malenco rocks underwent initial serpentinisation in the presence of oceanic water, although rocks nearest to the Bergell intrusives display a different isotopic signature. This possibly indicates an influence of fluids associated with contact metamorphism, and implies that a free fluid-phase was present during the metamorphism and allowed the large-scale convective transfer of stable isotopes. All the ultramafic rocks in the area underwent regional metamorphism (Trommsdorff and Evans, 1974) to produce a schistose lithology with the low-grade, greenschist-facies assemblage of antigorite + olivine + diopside + chlorite + magnetite. The subsequent emplacement of the Bergell acid-intrusvie complex caused local contact metamorphism of the ultramafic rocks (Trommsdorff and Evans, 1972).

Mineralogical Magazine, September 1991, Vol. 55, pp. 367–377

According to these authors, the contact between the ultramafic and intrusive rocks (tonalites) is probably sub-vertical. Trommsdorff and Evans (1972) mapped four isograds in the ultramafic rocks (Fig. 1): (i) tremolite + olivine-in; (ii) olivine + talc-in; (iii) anthophyllite-in; (iv) enstatite-in; of these, the second was ascribed to the antigorite-breakdown reaction

$$\text{antigorite} = \text{olivine} + \text{talc} + H_2O \quad (A)$$

and is most relevant to this study.

Petrography and microprobe analysis of antigorite breakdown

Samples of ultramafic rock were collected along several traverses approximately perpendicular to the igneous contact. The observed assemblages in the system MgO–CaO–SiO_2–H_2O are identical to those described by Trommsdorff and Evans (1972). Chlorite and magnetite are common accessory minerals throughout the aureole and imply the presence of significant Al_2O_3 and Fe_2O_3. In order to study antigorite breakdown we concentrated on rocks close to the olivine + talc-in isograd. Three rocks will be described in detail, one from either side of the isograd and one from the isograd itself (Fig. 1).

Sample RWB13 (Map Reference: Swiss coordinates 779.6, 129.6) contains antigorite, olivine, tremolite, chlorite and magnetite. The rock possesses two planar fabrics imparted during regional metamorphism. A primary cleavage is defined by the sheet-silicates antigorite and chlorite and is folded by an oblique set of crenulations along which a weak, second cleavage is developed. Tremolite cuts across both cleavages and forms euhedral prisms and needles. Very fine-grained magnetite is dispersed evenly through the section. Olivine forms equant to slightly elongate grains 0.01 to 0.2 mm in diameter, trails of which are strung out along the first cleavage. Antigorite and chlorite form flakes up to 0.05 mm long. The tremolite is probably the only mineral entirely of contact-metamorphic origin as it is the only one which does not follow the cleavage; also, tremolite was not stable with olivine under the low-grade regional metamorphic conditions that produced the assemblage olivine + diopside + antigorite in rocks outside the aureole (Trommsdorff and Evans, 1972).

RWB12 (Map Ref. 779.5, 129.6) was collected about 100 m nearer to the igneous contact than RWB13 and contains antigorite, olivine, tremolite, magnetite, chlorite and talc. The cleavage is less well developed in this rock than in those farther from the igneous contact. Antigorite forms a mesh of interlocking, randomly oriented to subparallel sheaves and flakes less than 0.5 mm in size. Most of the olivine forms elongated masses of equant grains less than 0.1 mm in diameter but, locally, small isolated olivines have grown interstitially in relatively coarse patches of antigorite. Talc occurs as tiny grains interleaved with and dispersed within antigorite. Talc and tremolite are randomly oriented with respect to the remnant regional-metamorphic textures and are probably of contact metamorphic origin.

Rock RWB9 (Map Ref. 779.35, 129.6) contains olivine, talc, tremolite, chlorite and magnetite. Olivine forms large, polycrystalline masses composed of randomly oriented grains less than 0.1 mm in size. Patches of phyllosilicate separate the olivine masses and are composed of subparallel flakes, about 0.05 mm in length, of talc and subordinate chlorite. Tremolite and magnetite form tiny, euhedral grains dispersed throughout the sample.

In the three samples described above, the amount of antigorite decreases steadily to zero as the igneous contact is approached, the amount of talc increases from zero to up to 30% by volume and olivine increases from about 30% to about 70% by volume. These trends are consistent with observations on other rocks collected from near the olivine + talc-in isograd.

Mineral chemistry was determined by detailed electron microprobe analysis. A Cameca Camebax was operated at 15 kV and about 3 nA with an analysis time of 100 seconds in the energy-dispersive mode. A spot size of about 5 μm was used, although a smaller spot was occasionally employed when the fine-grained talc–antigorite intergrowth in RWB12 was analysed. Olivine, talc and antigorite analyses are presented in Table 1. It is noticeable that olivine becomes richer in the forsterite component in the order RWB13, RWB12 and RWB9, i.e. with increasing metamorphic grade. Also the spread of antigorite compositions is smaller in RWB12 than in RWB13; the average antigorite composition is richer in Mg for the rock closer to the igneous contact. Talc contains an appreciable amount of Al_2O_3 in some analyses. It is clear that these minerals partition Fe in the order talc < antigorite < olivine.

Transmission electron microscopy

Background. Antigorite contains 1:1 tetrahedral : octahedral layers parallel to (001). The layers reverse their orientation periodically and a corrugated structure results which has a large periodicity parallel to the *a*-axis (Zussman, 1954).

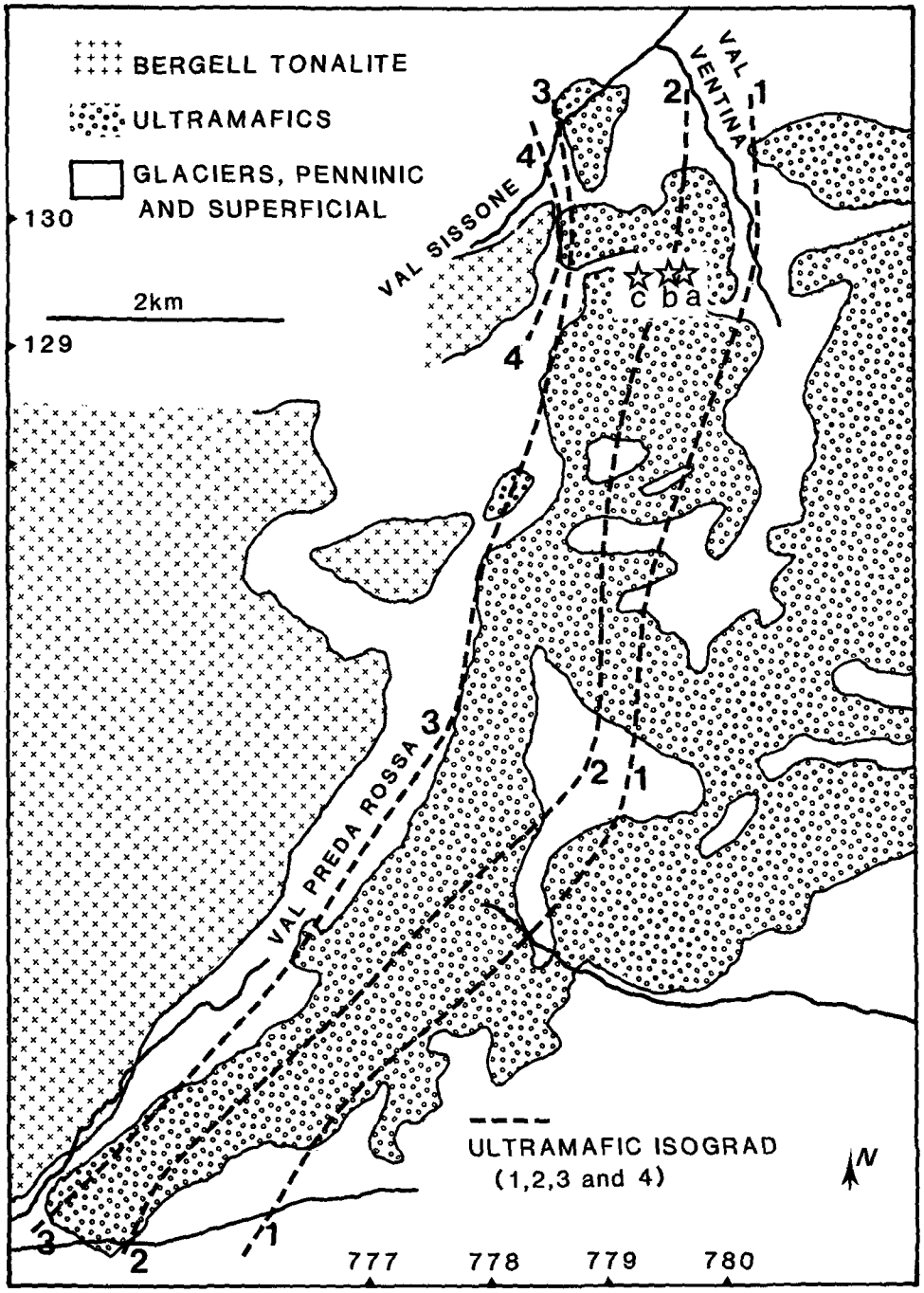

FIG. 1. Locality map of the Bergell aureole illustrating the intrusive rocks and the approximate distribution of ultramafic rocks. The isograds are drawn after data from Trommsdorff and Evans (1972) and Trommsdorff (pers. comm.). 1. tremolite + olivine-in; 2. olivine + talc-in; 3. anthophyllite-in; 4. enstatite-in. The position of rocks RWB13, RWB12 and RWB9 are illustrated by stars and are labelled a, b and c, respectively.

Mellini *et al.* (1987) made a detailed TEM study of the structural and chemical changes that occur in antigorites with increasing metamorphic grade. They found that, with increasing temperature, the antigorite becomes richer in SiO_2 and the superlattice periodicity decreases from about 6.0 nm at 250 °C to about 3.5 nm at 550 °C. Crystal size and superlattice homogeneity were found to increase and disorder and defect density were found to decrease with increasing grade.

Techniques. Samples were extracted from doubly-polished 20 μm optical thin-sections and were thinned to perforation in an Ion Tech ion mill operating at 5 kV. A Philips EM430 electron microscope was used and was operated at 300 kV. It was fitted with an EDAX X-ray detector system and a Gatan image intensifier. The maximum total magnification on the visual display unit was about 20 million times. This allowed simple focussing and correction of objective lens astigmatism to be carried out rapidly and accurately. The double-tilt goniometer was fitted with a beryllium cup and specimen-containing ring which reduced the generation of spurious X-rays. As the serpentine minerals are notoriously susceptible to decomposition and vitrification under electron bombardment, it was necessary to orient the sample correctly and adjust the focus and astigmatism on an *adjacent* area, and then move quickly to the area of interest and record the image. The high voltage greatly reduced the rate of beam damage and increased the area of specimen that was transparent to the electron beam compared to microscopy at 100 or 120 kV. X-ray analysis of mineral grains in the TEM was performed routinely for rapid mineral identification, but quantitative analysis was impossible owing to the high rates of beam damage.

Antigorite from talc-free contact rocks. A detailed TEM study of the antigorite in RWB13 provided an indication of the nature of the antigorite before breakdown. This sample corresponds to almost the highest temperature antigorites studied by Mellini *et al.* (1987).

The antigorite forms randomly oriented intergrowths of grains up to 50 nm wide and 200 nm long. The grains tend to be elongated along [100] (Fig. 2). The superlattice, which is clearly seen in Figs. 2 and 3 contains superlattice 'dislocations' (arrowed in Fig. 3) and in some cases, crystals are

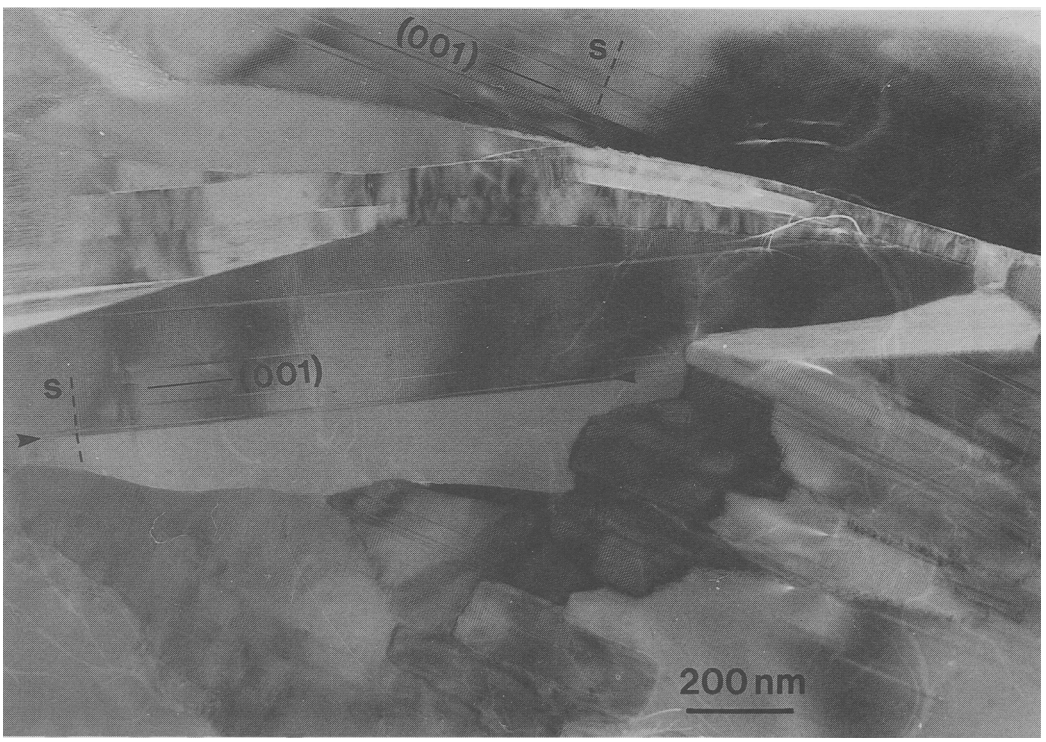

FIG. 2. Low-magnification, bright-field TEM image of antigorite from RWB13. The antigorite superlattice is clearly visible and is indicated by the dashed lines s. The central crystal is clearly twinned on (001) as shown by the change in orientation of the superlattice across the (arrowed) composition plane.

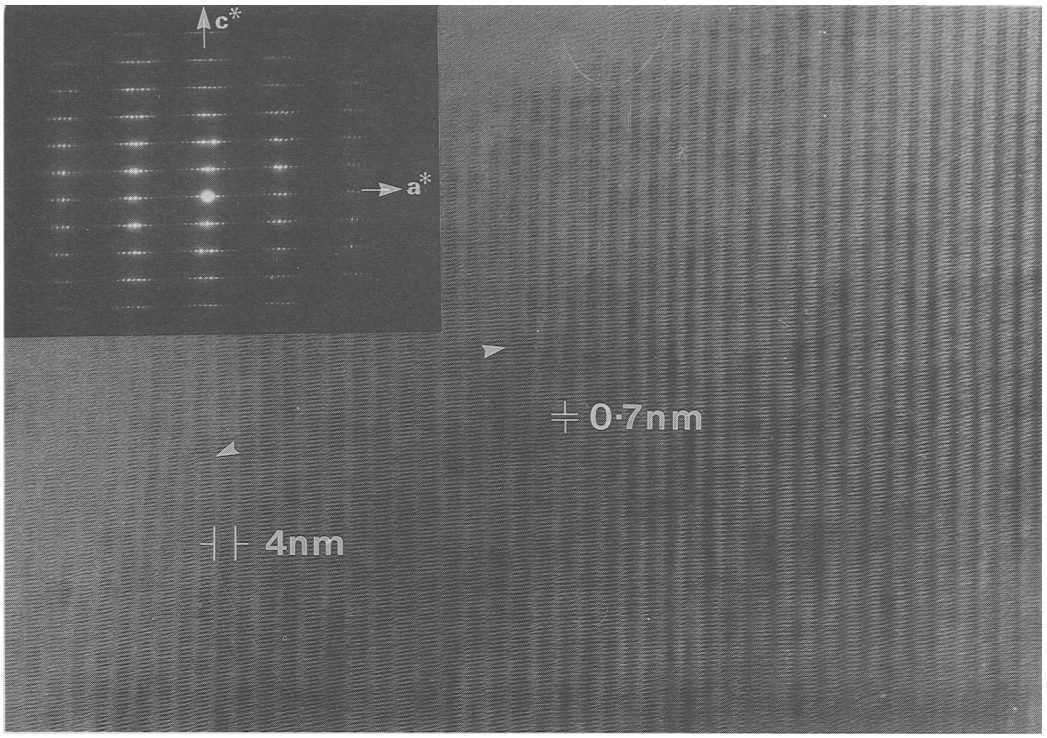

FIG. 3. High-resolution, bright-field [010] TEM image of antigorite in which the a-superlattice and the (001) planes are clearly visible. Notice the dislocations in the superlattice (arrowed) and the slight variation in the superlattice repeat. Inset: [010] electron-diffraction pattern of antigorite in which the superlattice spots are visible and correspond to a repeat of about 3.5 nm.

twinned on (001) (Fig. 3). Both these phenomena were described by Mellini *et al.* (1987). Apart from the slight variation in the superlattice repeat, the antigorite is highly ordered and is not intergrown with either of the other serpentine polytypes (compare Veblen and Buseck, 1979) or with other sheet silicates (compare Livi and Veblen, 1987) (Fig. 3). The superlattice repeat of 3.5 nm is typical of high-temperature polysomes. A diffraction pattern is shown in the inset to Fig. 3; notice that the $a^*_{\text{superlattice}}$ is parallel to a^*_{lattice}, as is usual for high-temperature antigorites (Mellini *et al.*, 1987). Stacking disorder along the *y*-axis is apparent in [100] images of the antigorite and is typical of many sheet-silicates (e.g. chlorite, micas).

TEM of talc-bearing rocks: In order that the interfaces between minerals in RWB12 (the sample containing antigorite, talc and olivine) could be studied, thin foils containing both reactant and product were prepared. Although thin foils with large electron-transparent areas containing talc and antigorite were easily prepared due to the very similar ion-thining rates of these two minerals, our attempts to study antigorite–olivine and talc–olivine interfaces were severely hampered by the great difference in the ion-thinning rates of these pairs of minerals.

Talc occurred as the 1M polytype with a 0.9 nm basal spacing rather than the usual 2M polytype with the 1.8 nm basal spacing described by Deer *et al.* (1962). Talc crystallography is analogous to that of muscovite, which can also occur as either a 2M or 1M polytype. Akizuki and Zussman (1978) have previously described a 1M talc polytype.

All talc grains are less than 2 μm wide and 5 μm long. The majority (about two thirds), are apparently randomly distributed in the antigorite matrix, but as the talc grains in question are large compared with the antigorite grains, it is impossible to tell where they nucleated. The rest of the talc grains are oriented with respect to the antigorite (Fig. 4), as first described by Veblen and Buseck (1979). The habit plane is normally approximately (001) for both minerals and the two phases are coherent, as shown by the diffraction pattern (inset, Fig. 4) and the lack of interfacial dislocations. In one example of a

stepped interface (Fig. 5) the (001) lattice planes are continuous across the steps, although there is a slight change in orientation of the planes.

The lattice orientation of the two phases in parallel intergrowth is (inset, Fig. 4):

$$(001)a \,//\, (001)t;$$
$$[100]a \,//\, [100]t$$

where the subscript a refers to antigorite and t refers to talc. In this orientation relationship the respective close-packed planes and close-packed directions are parallel in the two phases.

The diffraction patterns of both phases show streaks parallel to c^* for reciprocal lattice rows with $k \neq 3n$ (inset, Fig. 4). This is the result of the stacking disorder on (001) planes, that is visible in [100] images. It involves a fault vector of $b/3$.

Discussion

Chemistry of antigorite decomposition. The results described above show that talc formed by the breakdown of antigorite. However, the observation that the olivine + talc-in and antigorite-out isograds do not coincide implies that reaction A, which is univariant in the simple MgO–SiO_2–H_2O (MSH) system, is not discontinuous in the rocks. The most likely explanation for this is the presence of non-MSH components in one or more of the reactant or product phases. These components would have the effect of increasing the thermodynamic variance of the system. One possibility is that the fluid phase contains a significant concentration of components other than H_2O; CO_2 is the most likely culprit, but it is doubtful that much CO_2 was present as the serpentinites outside the aureole contain little or no carbonate. A more likely factor is the presence of non-MSH components in the silicate minerals. As reported in Table 1, these minerals contain FeO and, in the case of talc and antigorite, minor Al_2O_3. In order to represent the system graphically we have assumed water and chlorite to be excess components and have projected from them onto part of the SiO_2–MgO–FeO plane (Fig. 6). Chlorite is present in all the three analysed rocks and, to a first approximation, has a constant composition of $Mg_{10.2}Fe_{0.2}Al_{3.2}Si_{6.4}O_{20}(OH)_{16}$.

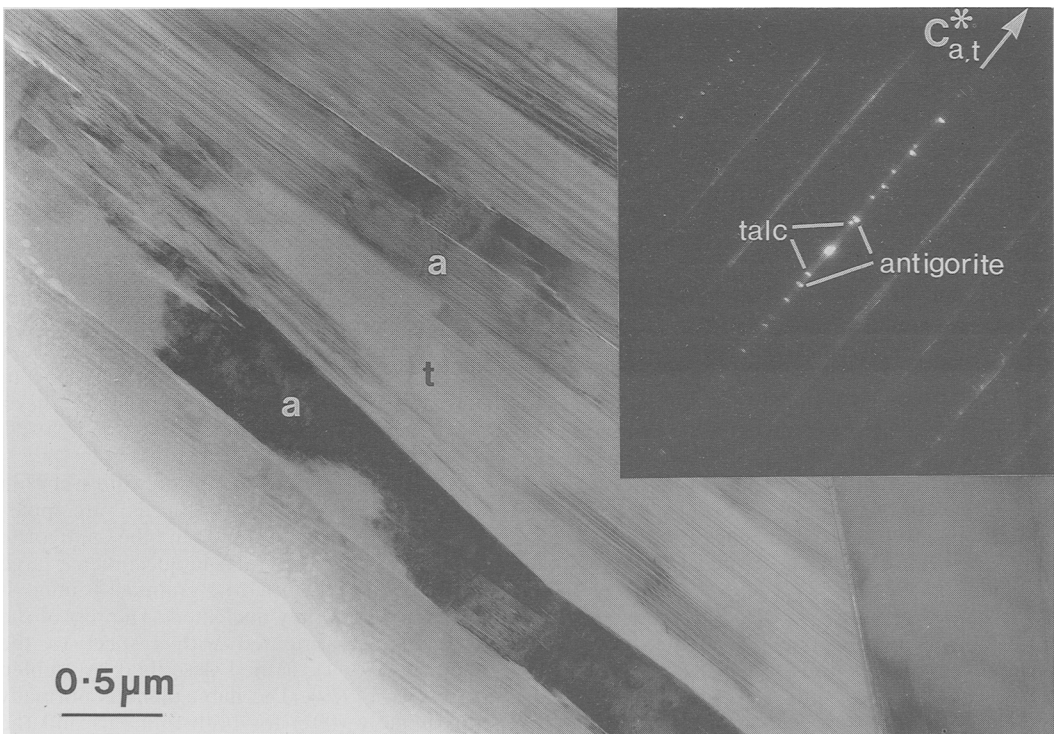

FIG. 4. TEM image of intergrown talc (t) and antigorite. The mutual interfaces are approximately parallel to (001) in both cases. Inset: [100] electron-diffraction pattern of antigorite and intergrown talc which is correctly oriented with respect to the micrograph. The phases share a common (001) lattice plane and are coherent. Sample RWB12.

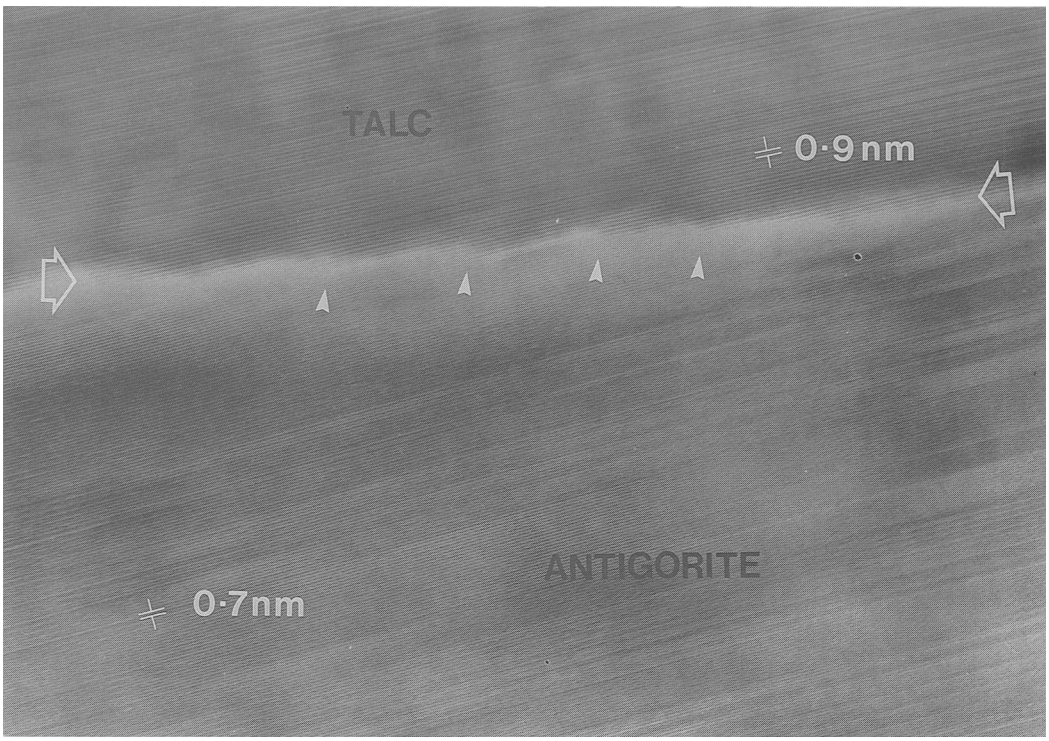

FIG. 5. High-resolution, bright-field TEM image of part of an antigorite–talc interface in RWB12, illustrating that a strong degree of continuity between the two mineral structures was maintained during the reaction. Note that the (001) planes of both minerals are sub-parallel and that the interface itself (large arrows) is oblique to (001) and has steps (small arrows) across which the talc and antigorite layers appear to be continuous.

The equilibrium assemblage antigorite + talc + olivine + chlorite (+ hydrous fluid) in RWB12 is represented by an antigorite–talc–olivine three-phase triangle (Fig. 6). Because the antigorite composition plots on the Mg-side of the olivine–talc tie-line, the antigorite will have become progressively richer in Mg relative to Fe as the reaction proceeded, causing the three-phase triangle to move across progressively more magnesian bulk compositions with increasing temperature. The role of alumina is not apparent from the projection. Because the antigorite is more aluminous than either talc or olivine, an aluminous component must be produced by the reaction. This could either be a Tschermak exchange-component or a separate, aluminous phase such as chlorite. The fact that chlorite is a common accessory either side of the olivine + talc-in isograd implies that the coexisting phases are already alumina-saturated and that the second possibility is correct. Thus the reaction producing talc from antigorite is (Mg, Fe)-continuous and may best be represented by the equation:

$$\text{antigorite} \rightarrow MgFe_{-1} + \text{talc} + \text{olivine} + \text{chlorite} + H_2O. \quad \text{(B)}$$

The volume of chlorite produced would have been very small compared with other product phases. Many authors, such as Springer (1974), Frost (1975), Arai (1975), Matthes and Knauer (1981) and Pinsent and Hirst (1977), as well as Trommsdorff and Evans (1972), have ascribed antigorite decomposition in contact and regional metamorphic environments to reaction A. This interpretation is clearly misleadingly simple and ignores the presence of minor other components such as Fe and Al. The presence of FeO also makes the above reaction composition-dependent, so that the olivine + talc isograd does not necessarily correspond to an isotherm.

Crystallography of antigorite breakdown. The structures of antigorite and talc contain layer subunits that are identical parallel to their (001) planes. It is not, therefore, surprising that the two phases often have an orientation relationship in which these two planes and the equivalent close-

Table 1. Microprobe analyses of olivine, antigorite and talc.

OLIVINE

Oxides	RWB13 OL1	RWB13 OL2	RWB13 OL3	RWB13 OL4	RWB12 OL1	RWB12 OL2	RWB12 OL3	RWB12 OL4	RWB9 OL1	RWB9 OL2	RWB9 OL3	RWB9 OL4
SiO2	41.23	41.78	42.29	41.76	41.35	41.11	42.26	42.88	41.63	42.05	42.00	42.71
FeO	13.62	13.51	13.80	14.54	7.95	7.12	9.49	8.86	8.17	8.41	8.31	6.53
MnO	0.35	0.51	0.39	0.45	0.23	0.53	0.34	0.22	0.00	0.00	0.00	0.27
MgO	45.67	45.55	46.44	46.01	48.93	49.18	48.76	49.45	47.88	48.87	49.31	49.13
Total	100.82	101.34	102.92	102.77	98.46	98.00	100.85	101.41	98.08	99.39	99.61	98.63
Formula	4(O)	4(O)	4(O)	4(O)	4(O)	4(O)	4(O)	4(O)	4(O)	4(O)	4(O)	4(O)
Si	1.01	1.01	1.02	1.01	1.01	1.02	1.02	1.02	1.03	1.03	1.02	1.02
Fe	0.28	0.27	0.28	0.29	0.16	0.15	0.19	0.18	0.17	0.17	0.17	0.13
Mn	0.01	0.01	0.01	0.01	0.01	0.01	0.01	0.01	0.00	0.00	0.00	0.01
Mg	1.68	1.65	1.67	1.67	1.79	1.83	1.75	1.76	1.76	1.76	1.78	1.77
Total	2.98	2.94	2.98	2.98	2.97	3.01	2.97	2.97	2.96	2.96	2.97	2.93
Mg/(Mg+Fe)	0.86	0.84	0.86	0.85	0.92	0.92	0.90	0.91	0.92	0.92	0.92	0.93

	ANTIGORITE									TALC			
Oxides	RWB13 ANT1	RWB13 ANT2	RWB13 ANT3	RWB13 ANT4	RWB13 ANT5	RWB12 ANT1	RWB12 ANT2	RWB12 ANT3	RWB12 ANT4	RWB12 TALC1	RWB12 TALC2	RWB12 TALC3	RWB9 TALC1
SiO2	43.38	43.88	43.54	41.01	40.70	45.41	45.51	45.69	45.61	62.42	64.69	62.85	58.76
Al2O3	4.45	4.53	5.00	3.84	4.87	1.83	1.14	1.51	1.95	0.36	0.00	0.00	0.48
FeO	4.99	5.16	5.05	4.55	4.63	3.10	3.41	3.32	3.28	1.28	1.19	0.99	0.78
MnO	0.00	0.22	0.00	0.00	0.00	0.00	0.00	0.00	0.00	0.00	0.00	0.27	0.00
MgO	36.84	37.51	37.15	35.77	36.77	38.22	38.37	38.36	36.98	29.75	29.45	29.71	27.75
Total	89.53	91.66	91.36	85.21	86.56	88.90	88.73	88.28	88.23	93.81	95.34	93.83	87.87
Formula	7(O)	7(O)	7(O)	7(O)	7(O)	7(O)	7(O)	7(O)	7(O)	11(O)	11(O)	11(O)	11(O)
Si	1.97	1.96	1.95	1.97	1.91	2.06	2.07	2.07	2.08	4.02	4.07	4.02	4.03
Al	0.23	0.24	0.26	0.22	0.27	0.09	0.06	0.08	0.10	0.02	0.00	0.00	0.04
Fe	0.19	0.19	0.19	0.18	0.18	0.12	0.13	0.13	0.13	0.07	0.07	0.06	0.05
Mn	0.00	0.01	0.00	0.00	0.00	0.00	0.00	0.00	0.00	0.00	0.00	0.02	0.00
Mg	2.48	2.49	2.48	2.56	2.54	2.59	2.61	2.60	2.52	2.86	2.76	2.84	2.84
Total	4.87	4.89	4.88	4.93	4.90	4.86	4.87	4.88	4.83	6.97	6.90	6.94	6.96
Mg/(Mg+Fe)	0.93	0.93	0.93	0.93	0.93	0.96	0.95	0.95	0.95	0.98	0.98	0.98	0.98

packed directions within them are parallel. Such an orientation relationship minimises the strain and surface energy components of the free-energy change at nucleation and is common in reactions involving solids.

The apparently *unoriented* grains of talc within partially reacted antigorite aggregates have probably totally replaced the antigorite grains in which they nucleated; the evidence of the orientation relationship has been obliterated.

Olivine bears no apparent orientation relationship to the parent antigorite. As the structures of these two phases enjoy some similarities, an orientation relationship would be expected and has been reported by Sousa Santos and Yada (1983) for olivine formed by rapid heating of antigorite.

The absence of an oriented reaction between antigorite and olivine in the Bergell sample RWB12 could be due to the abundance of olivine in the rock before antigorite breakdown. Olivine is common in rocks down-grade of the olivine + talc-in isograd (e.g. RWB13) and the new olivine could have grown on the pre-existing grains. This interpretation requires there to have been rapid and simple communication between the sites of antigorite decomposition and olivine growth. The work of Burkhard and O'Neil (1988) implies the presence of a free fluid-phase that originated, at least in part, from the crystallising pluton. Substantial quantities of hydrous fluid could also have been generated in the inner aureole by dehydration of antigorite, talc and anthophyllite. Conventional wisdom states that metamorphic fluids are held in the semi-amorphous, grain-boundary region. This fluid phase could facilitate the rapid diffusive interaction between the reacting antigorite and the olivine because diffusion along wet grain boundaries is much faster than along dry ones (Rubie, 1986).

Conditions of metamorphism. Trommsdorff and Evans (1972) used previous data to estimate

that the pressure in the aureole was not greater than 2 kbar. A more precise estimate is not possible because of the absence of relevant, suitable mineral geobarometers in this set of rocks.

From the experimental work of Evans *et al.* (1976), we know that, at 2 kbar, antigorite reacts to produce olivine and talc at about 515 °C in the pure MSH system. The fluid phase present during the metamorphism in the Bergell aureole was probably almost pure H_2O as no carbonate minerals are present in the ultramafic rocks. Also, at 2 kbar, serpentine is unstable with respect to magnesite + talc at $XH_2O/(XCO_2 + XH_2O)$ values less than 0.94 (Johannes, 1967, 1969). Thus the maximum possible decrease in the equilibrium temperature of reaction (A) on account of CO_2 dilution is very small (see also Trommsdorff and Evans, 1977), and is probably about 6 °C (Johannes, 1969). More important, potentially, is the influence of FeO. Because the olivine + talc assemblage has a lower Mg/Fe ratio than coexisting antigorite (Fig. 6*b*), the equilibrium temperature of the natural assemblage would have been lower than in the pure MSH system. Taking the means of the tabulated antigorite, olivine and talc analyses for sample RWB12 (Table 1) as representative of equilibrium compositions, and using the following simple ideal ionic mixing models:

$$a_a = (X_{Mg})^3;\ a_t = (X_{Mg})^3;\ a_{fo} = (X_{Mg})^2$$

we obtain values of 0.83, 0.88 and 0.83 for the activities of end-member antigorite, talc and forsterite, respectively. When the Powell and Holland (1988) dataset is used to calculate the chrysotile version of equilibrium (A) for these activities, we obtain a temperature only 4 °C lower than the equilibrium temperature in the pure MSH system.

Thus, although we have shown that the reaction under consideration would occur over a range of temperatures, that range would not have been great (of the order of 10 °C) and would have been near to the conditions of breakdown of

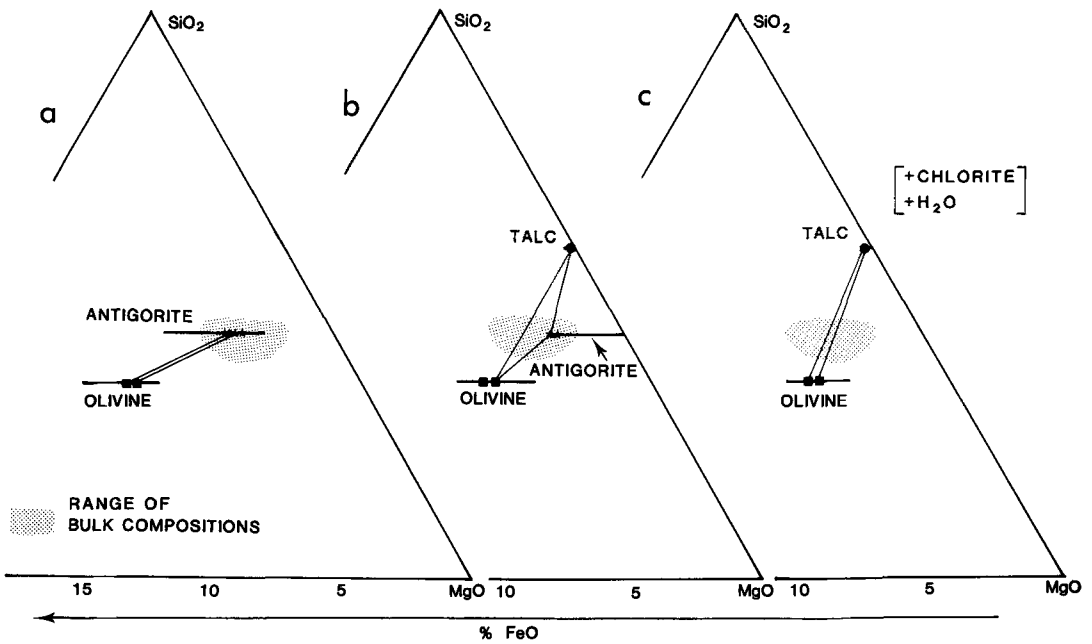

FIG. 6. Chemographic projection from water and chlorite (composition given in the text) onto the SiO_2–MgO–$FeMg_3O_4$ plane in the FMASH system. (a) Relatively low-grade sample RWB13; (b) Intermediate-grade sample RWB12; (c) Relatively high-grade sample RWB9. The shaded areas represent the range of bulk rock compositions given by Trommsdorff and Evans (1972). Note that (i) antigorite, talc and olivine coexist in RWB12, with the antigorite composition lying to the Mg side of the talc-olivine tie-line, (ii) the antigorite composition has higher Mg/(Mg + Fe) at higher grade, and (iii) both the antigorite–olivine and olivine–talc tie lines become steeper with increasing grade.

antigorite in the pure MSH system, at a temperature slightly higher than 500 °C.

The overstep of the reaction boundary was probably small because the heating rate was low and the activation energies for nucleation of the reaction products were low. Olivine nucleation was not necessary, the strain- and surface- energies for nucleation of talc were low and diffusion between the various sites of reaction was facilitated by the grain boundary fluid.

Conclusions

1. Antigorite decomposition in the Bergell aureole occurred by a continuous reaction over a small range of temperatures close to 500 °C at *ca.* 2 kbar. In addition to major olivine and talc, the reaction possibly also generated minor amounts of chlorite.
2. The persistence of antigorite immediately upgrade of the olivine + talc isograd was not due to metastability. Rather, it was caused by the minor component FeO increasing the variance of the assemblage antigorite + olivine + talc + fluid.
3. Talc and antigorite bear an orientation relationship to one another which minimises the strain and surface energies during nucleation.
4. Olivine nucleation was not necessary because this phase was present in the rocks before the onset of antigorite decomposition.
5. The abundance of fluids in the aureole allowed easy chemical communication between the site of progressive antigorite breakdown and olivine growth and probably allowed convective heat transfer.
6. Antigorite has a small superlattice repeat before decomposition and has a low content of crystallographic defects, including twins and superlattice dislocations. This microstructure is in agreement with the work of Mellini *et al.* (1987) who found that, at a temperature of about 500 °C, the superlattice repeat and defect content of antigorite were small.

Acknowledgements

We thank Ian Brough, Graham Cliff and Peter Kenway for assistance with the TEM work. Steve Caldwell and Steve Mills showd great care in preparing the specimens for TEM. The paper has benefitted from constructive comments from M. Mellini and an anonymous reviewer. R. H. W. acknowledges an N.E.R.C. studentship.

References

Akizuki, M. Zussman, J. (1978) The unit cell of talc. *Mineral. Mag.*, **42**, 107–10.

Arai, S (1975) Contact metamorphosed dunite-harzburgite complex in the Chugoka district, Western Japan. *Contrib. Mineral. Petrol.*, **52**, 1–16.

Brearley, A. J. (1987) A natural example of the disequilibrium breakdown of biotite at high temperature: TEM observations and comparison with experimental kinetic data. *Mineral. Mag.*, **51**, 93–106.

Burkhard, D. J. M. and O'Neil, J. R. (1988) Contrasting serpentinisation processes in the Eastern Central Alps. *Contrib. Mineral. Petrol.*, **99**, 498–506.

Deer, W. A., Howie, R. A., and Zussman, J. (1962) *Rock forming minerals*, Vol. 3, Sheet-silicates. Longmans.

Dietrich, V., Vaugnat, M., and Bertrand, J. (1974) Alpine metamorphism of mafic rocks. *Schweiz. Mineral. Petrogr. Mitt.*, **54**, 291–333.

Evans, B. W., Johannes, W., Oterdoom, H., and Trommsdorff, V. (1976) Stability of chrysotile and antigorite in the serpentinite multisystem. *Ibid.*, **56**, 79–93.

Frost, B. R. (1975) Contact metamorphism of serpentinite, chlorite blackwall and rodingite at Paddy-Go-Easy Pass, Central Cascades, Washington. *J. Petrol.*, **16**, 272–313.

Johannes, W. (1967) Zur Bildung und Stabilität von Forsterit, Talk, Serpentin, Quarz und Magnesit im System MgO, SiO_2, H_2O, CO_2. *Contrib. Mineral. Petrol.*, **15**, 233 –50.

—— (1969) An experimental investigation of the system MgO–SiO_2–H_2O–CO_2. *Am. J. Sci.* **267**, 1083–104.

Livi, K. J. T. and Veblen, D. R. (1987) 'Eastonite' from Easton, Pennsylvania: a mixture of phlogopite and a new form of serpentine. *Am. Mineral.*, **72**, 113–25.

Matthes, S. and Knauer, E. (1981) The phase petrology of the contact metamorphism serpentinite near Ebendorf, Oberpfalz, Bavria. *Neues Jahrb. Mineral. Abh.*, **141**, 59–89.

Mellini, M., Trommsdorff, V., and Compagnoni, R. (1987) Antigorite polysomatism: behaviour during progressive metamorphism. *Contrib. Mineral. Petrol.*, **97**, 147–55.

Otten, M. T. and Buseck, P. R. (1987) TEM study of the transformation of augite to sodic pyroxene in eclogitised ferro-gabbro. *Ibid.*, **96**, 529–38.

Pinsent, R. H. and Hirst, D. M. (1977) The metamorphism of the Blue River ultramafic body, Cassiar, British Columbia, Canada. *J. Petrol.*, **18**, 567–94.

Powell, R. and Holland, T. J. B. (1988) An internally consistent thermodynamic dataset with uncertainties and correlations: 3. Applications to geobarometry, worked examples and a computer program. *J. Metamorphic Geol.*, **6**, 173–204.

Rubie, D. C. (1986) The catalysis of mineral reactions by water and restrictions on the presence of aqueous fluid during metamorphism. *Mineral. Mag.*, **50**, 399–416.

Sousa Santos, H. De. and Yada, K. (1983) Thermal transformation of antigorite as studied by electron optical methods. *Clays Clay Minerals*, **31**, 241–50.

Springer, R. K. (1974) Contact metamorphosed ultramafic rocks in the western Sierra Nevada foothills, California. *J. Petrol.*, **15**, 160–95.

Trolliard, G., Boudeulle, M., Lardeaux, J. M. and

Potdevin, J. L. (1988) Contrasted modes of amphibole development in coronitic metagabbros: TEM investigation. *Phys. Chem. Minerals*, **16**, 130–9.

Trommsdorff, V. and Evans, B. W. (1972) Progressive metamorphism of antigorite schists in the Bergell tonalite aureole (Italy). *Am. J. Sci.*, **272**, 423–37.

———(1974) Alpine metamorphism of peridotitic rocks. *Schweiz. Mineral. Petrogr. Mitt.*, **54**, 333–52.

———(1977) Antigorite–ophicarbonates: contact metamorphism in Val Malenco, Italy. *Contrib. Mineral. Petrol.*, **72**, 301–12.

Veblen, D. R. and Buseck, P. R. (1979) Serpentine minerals: intergrowths and new combination structures. *Science*, **206**, 1398–400.

Wayte, G., Worden, R. H., Droop, G. T. R., and Rubie, D. C. (1989) Disequilibrium breakdown of plagioclase during high pressure metamorphism: the role of infiltrating fluid. *Contrib. Mineral. Petrol.*, **101**, 426–37.

Worden, R. H., Champness, P. E., and Droop, G. T. R. (1987) Transmission electron microscopy of the pyrometamorphic breakdown of phengite and chlorite. *Mineral. Mag.*, **51**, 107–21.

———(1988) The mechanism of the thermal decomposition of sheet-silicates in rocks. Phase Transformations '87, 614–7. Institute of Metals, London.

Zussman, J. (1954) Investigation of the crystal structure of antigorite. *Mineral. Mag.*, **30**, 498–512.

[*Revised manuscript received 25 March 1991*]